JOURNAL OF AIRCRAFT
Vol. 33, No. 1, January–February 1996

# Aeroelastic Behavior of Composite Plates Subject to Damage Growth

Thomas W. Strganac* and Young Ik Kim†
*Texas A&M University, College Station, Texas 77843-3141*

**A study of the aeroelastic response of damaged composite plates is presented. The plates considered are those that undergo damage on a slow or rapid time scale due to the natural progression of microcracks in the composite structure. Dynamic characteristics are unique to the coupled damage/aeroelastic system and are developed as part of the solution methodology. The aeroelastic response is shown to be highly dependent upon the distribution and accumulation of damage, and the importance of the interdependence of aeroelastic stability and damage is established. The aeroelastic stability boundary evolves with the growth of damage and the results show the need to develop damage as part of the solution.**

## Introduction

AEROELASTICITY is the time-dependent interaction between aerodynamic, inertial, and structural forces. Typically, the elastic forces of the structure are assumed to behave in a linear manner and the stiffness of the structure is assumed to remain constant for the life of the structure. Although composite materials are used for aircraft applications as these materials provide lightweight, response-tailored structures, microstructural damage is both inherent and unavoidable in these materials. Sources of damage include matrix cracking, delamination, fiber breakage, or fiber–matrix debonding. Investigations to characterize damage have been quite active resulting in several analytically and experimentally based damage models. The influence of damage accumulation on the response of aeroelastic systems, including the aeroelastic stability of this evolving structure, is of interest. This evolution is the result of degradation of the structure due to the naturally occurring progression of damage and the damage accumulation is dependent upon the aeroelastic history of the structure.

Several studies, such as the efforts of Dowell[1] and Gray et al.,[2] have addressed the specific case of nonlinear panel flutter of plate-like structures, but the authors are aware of no studies that address the aeroelastic performance of composite structures with microstructural damage. Dowell[3] described the change in the aeroelastic stability arising from the degradation of an isotropic plate structure due to fatigue. Dowell suggested that nonlinear flutter analysis would permit the prediction of the fatigue life of the associated plate structure. Dowell further suggested that conventional fatigue data could be used for estimating the fatigue life of the plate structure specifically at flutter conditions; however, this effort did not address the relationship between the displacement-dependent loads associated with aeroelastic behavior and the growth of fatigue loads. Xue et al.[4] studied the fatigue life of beams with thermal effects. Frequencies and stresses for the limit-cycle behavior of these structures were determined for several thermal loading conditions. The critical dynamic pressure at which flutter occurred was found for various structural states throughout the fatigue-life history; these results show that infinite fatigue life was guaranteed below a certain dynamic pressure. Chen et al.[5] presented studies of panel flutter for thin cracked plates. The structure was limited to small displacement and a single crack case. A hybrid-displacement finite element was used in order to facilitate the singularity near the crack tip. The influence of the crack length and flow direction on the critical dynamic pressure was presented.

The results presented herein build upon the preliminary efforts previously described by Kim et al.[6] and Strganac et al.[7] Since the primary goal of this study is to contribute to the understanding of the behavior of aeroelastic systems with structural evolution, a simple aeroelastic model is used. The structure is represented by a composite laminate plate and piston theory is used to represent the unsteady aerodynamic loads. The model of microstructural damage for composite plates is also developed. Results are presented for two examples of aeroelastic systems with microstructural damage: 1) panel flutter of a composite plate and 2) bending-torsion flutter of a wing represented by a cantilevered composite plate.

## Theory

### Aeroelastic Equations

The equations of motion for the transverse response of a plate (Fig. 1) are

$$D\nabla^4 w + \rho \frac{\partial^2 w}{\partial^2 t} = p \tag{1}$$

where $D$ is the structural stiffness, $\rho$ is the material density, $p$ is the distributed aerodynamic load, and $w$ is the transverse displacement.

The aerodynamic loads are dependent upon the motion of the structure. Numerous models have been developed to de-

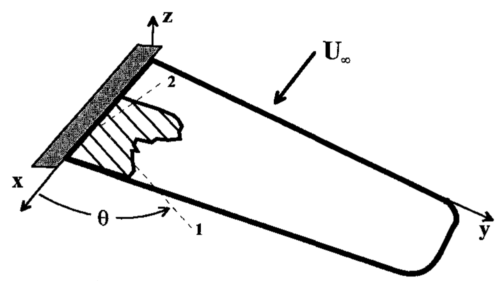


**Fig. 1 Aeroelastic response is predicted for a cantilevered composite laminate plate. The principal directions of the laminae are rotated by angle *θ* relative to the laminate plate.**

Received June 24, 1994; revision received June 5, 1995; accepted for publication July 11, 1995. 

*Associate Professor, Department of Aerospace Engineering. Associate Fellow AIAA.

†Graduate Research Assistant, Department of Aerospace Engineering. Member AIAA.

scribe unsteady aerodynamic loads. Examples include the vortex lattice method developed by Strganac and Mook,[8] which is appropriate for subsonic flow; the doublet lattice method developed by Albano and Rodden,[9] which is widely accepted for aeroelastic studies in the subsonic flow regime; and the efforts of Batina,[10] which provide a methodology for unsteady transonic flows. For the present study, these unsteady aerodynamic loads are determined by piston theory[11]

$$p = \frac{2q_\infty}{\sqrt{M_\infty^2 - 1}}\left[\frac{\partial w}{\partial x} + \frac{1}{U_\infty}\frac{(M_\infty^2 - 2)}{(M_\infty^2 - 1)}\frac{\partial w}{\partial t}\right] \tag{2}$$

where $q_\infty$ is the dynamic pressure (defined as $\rho_\infty U_\infty^2/2$), $M_\infty$ is the Mach number, $\rho_\infty$ is the air density, and $U_\infty$ is the flow velocity.

Piston theory is limited to hypersonic flow and/or hf motion, yet this theory provides a simple mechanism to model the unsteady aerodynamic loads on the plate. The aerodynamic loads are computed at a specific point on the lifting surface with no influence from any other point (no spatial dependence) and with no influence from the prior history of the motion (no temporal dependence). However, the aerodynamic loads are velocity and displacement dependent, and as such these loads introduce both damping-related forces and stiffness-related forces.

The governing equations for the aeroelastic response of plates with damage are derived in detail by Kim.[12] The equations for linear aeroelastic behavior of the plate are written as

$$\frac{1}{\omega_0^2}[\bar{M}]\{\ddot{W}\} + \frac{\bar{g}}{\omega_0}[\bar{C}_A]\{\dot{W}\} + [[\bar{K}_S] + \bar{\lambda}[\bar{K}_A]]\{W\} = \{G_A\} \tag{3}$$

where the overbar indicates nondimensional quantities, $[\bar{M}]$ is the mass matrix, the matrices $[\bar{C}_A]$ and $[\bar{K}_A]$ represent damping and stiffness contributions from the unsteady aerodynamic loads, $[\bar{K}_S]$ is the stiffness of the structure that includes the effect of damage and depends upon the prior load history, and $\{G_A\}$ is an external excitation due to forcing from disturbances such as gusts or turbulence. A reference frequency, aerodynamic parameter, and damping parameter are introduced in Eq. (3); these terms, respectively, are defined as

$$\omega_0 = \sqrt{D_R/\rho h a^4} \tag{4}$$

$$\bar{\lambda} = \frac{a^3}{D_R}\frac{2q_\infty}{\sqrt{M_\infty^2 - 1}} \tag{5}$$

$$\bar{g} = \sqrt{\frac{\bar{\lambda}\mu}{\sqrt{M_\infty^2 - 1}}\frac{M_\infty^2 - 2}{M_\infty^2 - 1}} \tag{6}$$

where $h$ is the plate thickness, $a$ is the reference length (chord of the plate), $D_R$ is the reference stiffness [defined as $E_2h^3$, where $E_2$ is the modulus in the 2 material direction (see Fig. 1)], and $\mu$ is the mass ratio [defined as $(\rho_\infty a/\rho h)$].

The governing equations [Eq. (3)] are solved in the time-domain to effectively include the interaction with the damage growth model. With this nondimensional form of the equations a nondimensional time is introduced such that $\tau = ta/U_\infty$. In addition, the system is examined in the frequency domain to identify the frequency and damping characteristics of the evolving structure. To this end, a solution for these equations of the form $\{W\} = \{\bar{W}\}e^{\Omega\tau}$ is assumed, where $\Omega = \delta \pm i\omega$, in which $\delta$ represents aperiodic motion and $\omega$ represents oscillatory motion. With this assumption, and ignoring the external loads $\{G_A\}$, the equations are

$$[[\bar{K}_S] + \bar{\lambda}[\bar{K}_A] - \kappa[\bar{M}]]\{\bar{w}\} = 0 \tag{7}$$

The eigenvalue $\kappa$ describes both frequency and damping characteristics that depend upon the flow conditions. The eigenvalue is defined as

$$\kappa = -(\Omega/\omega_0)^2 - \bar{g}(\Omega/\omega_0) = \kappa_R \pm i\kappa_I \tag{8}$$

Equation (7) and the associated eigenvalue reduces to a standard form representing the free vibration characteristics of the structure if the dynamic pressure is zero (i.e., $\bar{\lambda} = 0$). As the dynamic pressure is increased, two (or more) frequencies may tend to approach each other and the damping of the system goes to zero. $\bar{\lambda}_{CR}$ is defined as the critical dynamic pressure at which the coalescence of frequencies $\kappa_R$ occurs and $\bar{\lambda}_{FL}$ is defined as the flutter dynamic pressure at which the system damping $\kappa_I$ goes to zero. If the system damping is zero then $\Omega = \pm i\omega$; thus, from Eq. (8):

$$\kappa = \kappa_R \pm i\kappa_I = (\omega/\omega_0)^2 - i\bar{g}(\omega/\omega_0) \tag{9}$$

The terms in Eq. (9) lead to

$$\omega = \omega_0\sqrt{\kappa_R} \tag{10}$$

$$\omega = \omega_0\bar{g}\kappa_I \tag{11}$$

The damping parameter is found from Eqs. (10) and (11) as

$$\bar{g} = \kappa_I/\sqrt{\kappa_R} \tag{12}$$

Also, from Eq. (6) $\bar{g} \equiv \sqrt{\bar{\lambda}(\mu/M_\infty)}$ (for the case $M_\infty >> 1$), thus, the dynamic pressure at which flutter occurs is

$$\bar{\lambda}_{FL} = (M_\infty/\mu)(\kappa_I^2/\kappa_R) \tag{13}$$

In general, $\bar{\lambda}_{CR}$ is not equal to $\bar{\lambda}_{FL}$ since $\bar{\lambda}_{FL}$ depends upon the aerodynamic damping, $(\mu/M_\infty)$. Typically, $\bar{\lambda}_{FL}$ is greater than $\bar{\lambda}_{CR}$, but $\bar{\lambda}_{FL}$ approaches $\bar{\lambda}_{CR}$ as $(\mu/M_\infty)$ approaches zero.

**Damage Model for the Structure**

The damage model used in this study follows the general formulation given by Coleman and Gurtin[13] as described in their work on thermodynamics with internal state variables (ISV). The method proceeds from the assumption that ISVs can be implemented to describe the state of damage. A characteristic of the ISV approach is that an elastic medium with damage is treated as an equivalent homogeneous material. Damage effects are introduced at the ply level; thus, the ISV method is independent of the stacking sequence associated with the laminate.

The wing structure is modeled as a composite laminate plate as described by Jones.[14] The internal forces $\{N\}$ and moments $\{M\}$ are the result of the unsteady aerodynamic loads and are related to extension and flexure of the plate as

$$\begin{Bmatrix} \{N\} \\ \{M\} \end{Bmatrix} = \begin{bmatrix} [A^d] & [B^d] \\ [B^d] & [D^d] \end{bmatrix} \begin{Bmatrix} \{\varepsilon_L\} \\ \{\kappa_L\} \end{Bmatrix} \tag{14}$$

where the matrices $[A^d]$, $[B^d]$, and $[D^d]$ are the extensional, extension–flexure coupling, and flexural stiffness matrices, respectively. These stiffness terms incorporate damage; thus, the superscript $d$ is introduced to emphasize the presence of damage. The term $\{\varepsilon_L\}$ represents the local strain and the term $\{\kappa_L\}$ represents the local curvature.

The damage-dependent stiffness components ($[A^d]$, $[B^d]$, and $[D^d]$) of the laminate are found from the damage-dependent stiffness of each lamina. The stiffness of the lamina in the principal material directions is defined[14] as

$$[Q] = \begin{bmatrix} \dfrac{E_1^d}{1 - \nu_{12}^d\nu_{21}^d} & \dfrac{\nu_{12}^d E_2^d}{1 - \nu_{12}^d\nu_{21}^d} & 0 \\ \dfrac{\nu_{12}^d E_2^d}{1 - \nu_{12}^d\nu_{21}^d} & \dfrac{E_2^d}{1 - \nu_{12}^d\nu_{21}^d} & 0 \\ 0 & 0 & G_{12}^d \end{bmatrix} \tag{15}$$

where $E_1$, $E_2$, $\nu_{12}$, $G_{12}$, and $\nu_{21}$ $(=\nu_{12}E_2/E_1)$ are constitutive properties of the lamina. The subscript 1 indicates the fiber direction as illustrated in Fig. 1 and the subscript 2 indicates the direction normal to the fiber direction. These directions are related to the $x$-$y$ coordinate system of the plate by the angle $\theta$ shown in Fig. 1. Again, the superscript $d$ indicates the influence of damage.

The constitutive properties of the damaged lamina in the principle material directions are related to the properties of the undamaged lamina by

$$E_1^d = E_1 + 2\xi[C_3 + C_8(\nu_{12})^2 - C_{16}\nu_{12}] \tag{16}$$

$$E_2^d = E_2 + 2\xi[C_8 + C_3(\nu_{21})^2 - C_{16}\nu_{21}] \tag{17}$$

$$\nu_{12}^d = \nu_{12} + \xi\left(\frac{1 - \nu_{12}\nu_{21}}{E_2}\right)(C_{16} - 2C_8\nu_{12}) \tag{18}$$

$$G_{12}^d = G_{12} + 2\xi C_{13} \tag{19}$$

where $\xi$ is the damage parameter introduced by Talreja[15,16] to describe the density of damage at the ply level and the terms $C_3$, $C_8$, $C_{13}$, and $C_{16}$ are experimentally derived material constants.

The stiffness matrices in Eq. (14) are found by integrating the lamina contributions through the thickness of the plate

$$(A_{ij}^d, B_{ij}^d, D_{ij}^d) = \int \bar{Q}_{ij}^d(1, z, z^2)\,dz \tag{20}$$

where $\bar{Q}_{ij}^d$ is the stiffness of the lamina with damage in the $x$-$y$ coordinate system (see Fig. 1) and the subscripts indicate the element of the stiffness matrix. $\bar{Q}_{ij}^d$, which is a function of $E_1^d$, $E_2^d$, $\nu_{12}^d$, $G_{12}^d$, and $\theta$, is found in the conventional manner as described by Jones.[14] The stiffness matrix $[\bar{K}_S]$ of Eqs. (3) and (7) is derived from $[D^d]$ as described in detail by Kim.[12]

The damage parameter $\xi$ represents the crack density, the magnitude of which is subject to a damage growth law. $\xi$ is dependent upon the stress and frequency (or time) associated with the motion of the wing. The stress field depends upon the stacking sequence associated with the laminate as well as the unsteady aerodynamic loads. The model of damage growth incorporates the efforts of Talreja,[15,16] Allen et al.,[17-19] and Harris et al.[20] In general, the ISVs are described as

$$\dot{\alpha}_{ij}^p = \dot{\alpha}_{ij}^p(\varepsilon_{ij}, T, \alpha_{ij}^p) \tag{21}$$

where $\alpha_{ij}^p$ is the set of $p$ ISVs, $\varepsilon_{ij}$ is the strain, $T$ is the temperature, and the overdot represents the derivative with respect to time.

For the general case of material damage, the ISVs are defined as

$$\alpha_{ij}^p = \frac{1}{V_L}\int_S u_i n_j\,dS \tag{22}$$

where $V_L$ is the local volume in which homogeneity is assumed, $u_i$ is the crack-face displacement, and $n_j$ is the normal. More specifically, the damage growth law for matrix cracking is given as[21]

$$d\alpha_{22}^p = \frac{d\alpha_{22}^p}{dS} kG^n\,dN \tag{23}$$

where $\alpha_{22}^p$ is the ISV representing matrix cracking, $k$ and $n$ are material constants, $G$ is the strain energy release rate, $S$ is the crack surface, and $N$ is the number of cycles.

Further, the growth is expressed in terms of stress as

$$\frac{d\alpha_{22}^p}{dS} = C_m\bar{\sigma} \tag{24}$$

where $\bar{\sigma}$ is the average stress in the direction normal to the fiber direction ($\sigma_2$ for the lamina principal material directions) and $C_m$ is a material parameter. Also, $G = V_L\bar{\sigma}(d\alpha_{22}^p/dS)$, thus, the growth of matrix cracks is described by

$$\frac{d\alpha_{22}^p}{dN} = C_m^{(n+1)}kV_L^n\bar{\sigma}^{(2n+1)} \tag{25}$$

The ISV, $\alpha_{22}^p$, is directly related to the nondimensional damage parameter $\xi$.

## Results

The dynamic response of a plate with damage exposed to a flow is obtained by integrating Eq. (3) with respect to time (a nondimensional time is used, $\tau = ta/U_\infty$). In addition, computation of the stability parameters, which include the aeroelastic frequencies, mode shapes, and freestream conditions at which aeroelastic flutter occurs, is performed by eigenanalysis of Eq. (7). These stability parameters are found for a sufficient number of damage states (time steps) to adequately describe the flutter boundary. The integration and eigenanalysis continues until damage saturation occurs.

The aeroelastic response of a graphite epoxy composite (AS4/3502) plate is examined. Table 1 presents the constitutive properties of the material for several levels of damage as measured by $\xi$. The loss of stiffness due to damage primarily occurs in the direction normal (the 2 direction) to the fiber direction.

Material constants for the damaged composite plate, as derived from experimental measurements by Sanders et al.[22] include $C_3 = -0.627 \times 10^6$ psi, $C_8 = -0.329 \times 10^6$ psi, and $C_{16} = -0.564 \times 10^6$ psi ($C_{13} = 0$ due to symmetry of the laminate's stacking sequence). Other material properties include $\rho = 1.4488 \times 10^{-4}$ lb-s$^2$/in.$^4$, $G_{12} = 0.7 \times 10^6$ psi, $t = 0.00544$ in. An aerodynamic damping parameter of $\mu/M_\infty = 0.10$ and a gust loading of $G_A = 0.004 \sin(120\tau)$ is used in the simulations.

Initially, the aeroelastic characteristics of the plate model shown in Fig. 2 are examined.[6,7] This first study assumes a semi-infinite plate such that the plate model is reduced to that of a beam model. The aeroelastic frequencies are presented in Fig. 3 for two damage cases. In one case the damage is assumed to be uniformly distributed; in the second case the state of damage is determined according to the local stress associated with the response. Flutter is characterized by the

**Table 1 Lamina properties for damaged graphite epoxy**

| $\xi$ | $E_1$, psi | $E_2$, psi | $\nu_{12}$ |
|---|---|---|---|
| 0.00 | $19.80 \times 10^6$ | $1.45 \times 10^6$ | 0.30 |
| 0.10 | $19.76 \times 10^6$ | $1.33 \times 10^6$ | 0.29 |
| 0.20 | $19.71 \times 10^6$ | $1.20 \times 10^6$ | 0.27 |
| 0.30 | $19.67 \times 10^6$ | $1.08 \times 10^6$ | 0.25 |
| 0.40 | $19.63 \times 10^6$ | $0.96 \times 10^6$ | 0.22 |

**Table 2 Flutter conditions for the two damage cases**

| Case | Undamaged | Uniform distribution | Stress distribution |
|---|---|---|---|
| $\kappa_R$ | 4.37 | 4.14 | 4.05 |
| $\lambda_{CR}$ | 19.80 | 21.60 | 19.10 |

Note: $\xi_{AVG} = 0.167$.

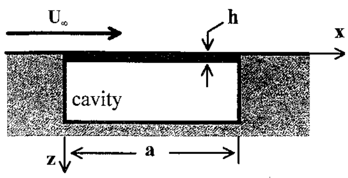


**Fig. 2 Panel flutter occurs as flow passes over a plate-like structure.**

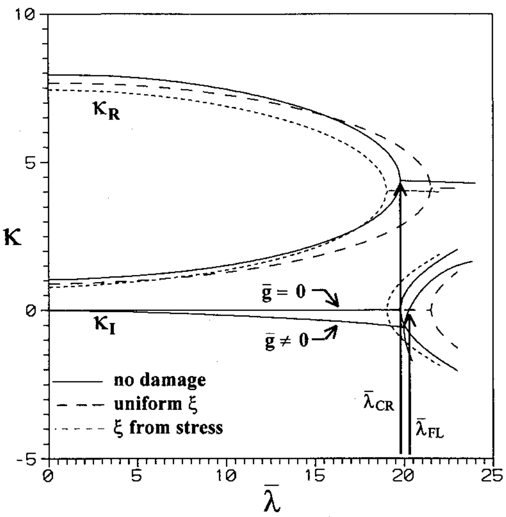


**Fig. 3 Complex eigenvalue $\kappa$ is found for increasing dynamic pressures. Vibration and stability characteristics depend upon the damage state of the evolving plate and the magnitude of the dynamic pressure. Results are shown for the plate without damage and for two damage cases used in the study. Results also show the effect of damping $\bar{g}$ on the prediction of flutter.**

coupling of two (or more) aeroelastic modes and the loss of damping in the system. The results presented in Fig. 3 show the aeroelastic frequencies associated with two modes for increasing dynamic pressures. At subcritical flow conditions these modes are separate and distinct, yet coupled, due to the presence of aerodynamic loads; however, these modes depend upon the flow conditions and at the onset of flutter these modes coalesce to form a single aeroelastic mode and frequency $\kappa_R$. In addition, the damping $\kappa_I$ of the system becomes zero. The flutter conditions for these two damage cases are presented in Table 2.

The results presented in Fig. 3 clearly show the need to develop the damage as part of the solution rather than assume a uniform loss of stiffness. The flutter conditions are apparently raised if uniform damage occurs as assumed in the first case; however, the second case shows that the flutter conditions are reduced if damage is found as part of the solution. The natural frequencies of the plate are dependent upon the stacking sequence of the laminae and the magnitude of damage, and the growth in damage is dependent upon the lamina orientation. Although the frequencies show a significant change due to damage, differences in the mode shapes due to damage are not remarkable.

Next, the aeroelastic response of a cantilevered composite plate, as depicted in Fig. 1, is examined. Predictions of aeroelastic response and the associated damage behavior depend upon the dynamic pressure. In the solution methodology described herein, the change in aeroelastic response is predicted for a specified dynamic pressure. In addition, a simple harmonic gust is used to excite the wing. The results presented in Fig. 4 show the stresses at the center of the plate due to the oscillatory forcing at two different dynamic pressures. The plate is a $[0/90]_s$ laminate. The stress level is larger for the flow conditions associated with the higher dynamic pressure; consequently, damage will occur at a faster rate as the dynamic pressure is increased. As shown in Fig. 5, the presence of damage will lead to failure. The results presented in Fig. 6 show that the time to failure increases as the margin between the dynamic pressure of the simulation and the dynamic pressure of flutter ($\bar{\lambda}_{FL} \cong 20.4$) increases. A lower bound of dynamic pressure exists at which the presence of damage will not lead to failure since significant stresses are not present.

The spatial and temporal distributions of the stress are required to model damage growth. The stress field is not uniform due to the distribution of the aerodynamic loads; thus, damage is not uniform and the accumulation of damage is concentrated in the region of the higher stresses associated with the dominate aeroelastic motion. To illustrate, the aeroelastic response of the laminate is predicted for $\bar{\lambda} = 18.0$ and the stress distribution for the plate laminae is shown in Fig. 7. This distribution shows the evolution of the stresses

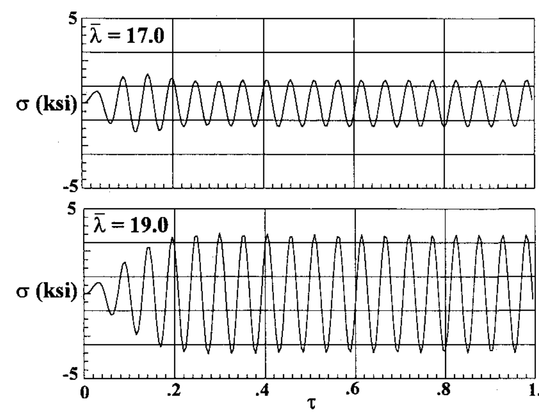


**Fig. 4 Damage growth depends upon the oscillatory stress field. The stress history is shown for the midpoint in the *x-y* plane of the plate for two dynamic pressures. The distribution of stresses depends upon the dynamic pressure, laminate properties, and damage state.**

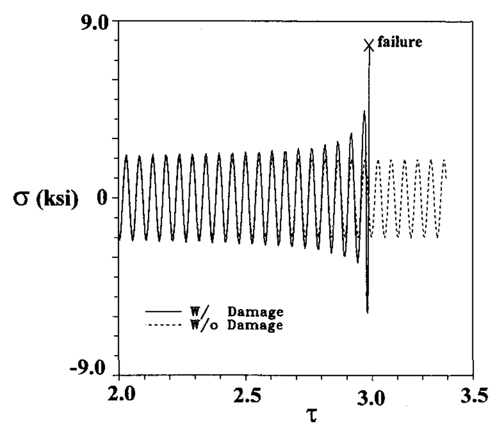


**Fig. 5 Aeroelastic loads are deformation dependent. Stresses will grow in the presence of damage and lead to failure. The spanwise stress is shown for the midpoint in the *x-y* plane of the plate for $\bar{\lambda} = 17.5$.**

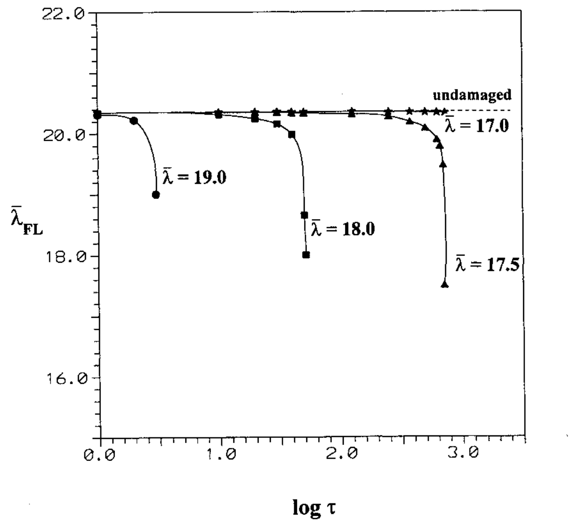


**Fig. 6 Time to failure depends upon the magnitude of the dynamic pressure. As the dynamic pressure approaches the critical dynamic pressure associated with flutter, the time to failure is reduced.**

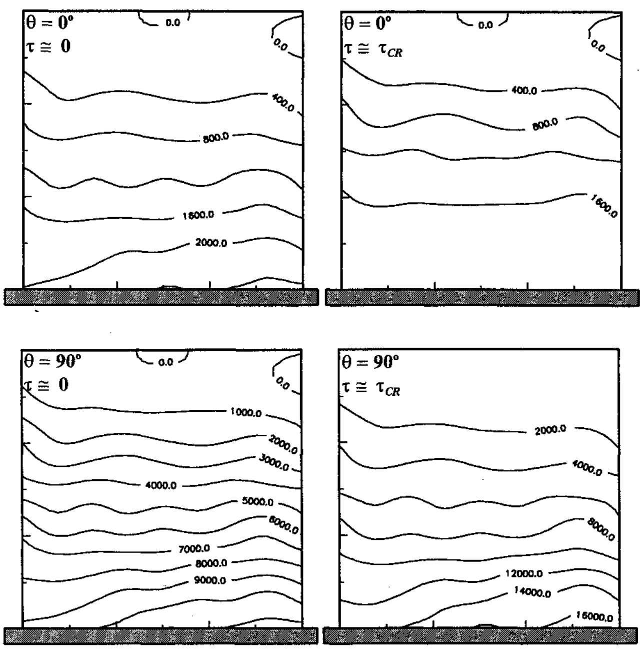


**Fig. 7 Stress state evolves due to the presence of damage and the unsteady aerodynamic loads. The spanwise stress field is shown for two laminae of a $[0/90]_s$ laminate.**

in the spanwise direction. The stresses in the chordwise direction are not shown as these stresses are significantly lower and show little change over time. The stresses in the outer lamina (primary stiffness in the chordwise direction) change little over time, whereas the stresses in the inner lamina (primary stiffness in the spanwise direction) show an appreciable growth over time. This increase in stress is the consequence of a change in the load path which resulted from the growth of damage. The distribution of damage for the outer lamina is shown in Fig. 8. The largest concentration of damage occurs near the clamped edge. In addition, the damage accumulates near the trailing edge due to the unsteady aerodynamic loads. Very little growth in damage occurs within the inner lamina as a consequence of the laminate design.

The evolution of the flutter boundary for the composite laminate plate is shown in Fig. 9. With damage growth, a reduction in the dynamic pressure at which flutter occurs is

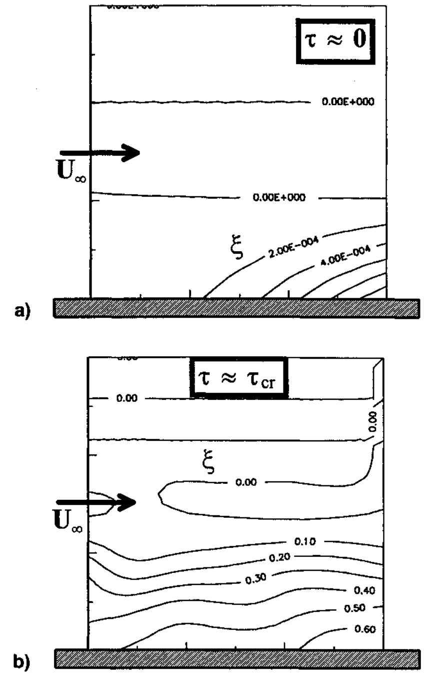


**Fig. 8 Change in structural stiffness is indicated by contours of $\xi$. The accumulation of damage is shown for an outer lamina of the plate: a) early damage of the plate and b) damage state immediately prior to flutter.**

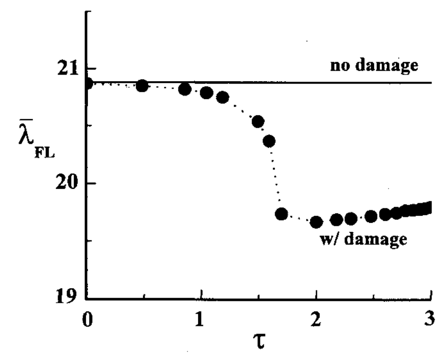


**Fig. 9 Flutter boundary is reduced due to the presence of damage. The reduction depends upon the magnitude of the operating dynamic pressure ($\bar{\lambda}$ = 18.0 for the case shown) and the properties of the laminate. The boundary plateaus as the stress field is redistributed over time.**

predicted. However, the boundary plateaus after the initial reduction as a consequence of a change in the stress distribution resulting from damage accumulation. The growth of damage, evolution of the stress field, and change in the flutter boundary depend upon the magnitude of the dynamic pressure at which the plate operates.

## Concluding Remarks

Many studies have been presented that examine the use of composite materials in aerospace systems; however, no studies are available that describe the dynamic response and stability of composite plates with naturally occurring damage in the presence of aeroelastic loads. Two cases have been presented: 1) panel flutter of a composite plate and 2) bending-torsion flutter of a wing modeled as a cantilevered composite plate. The dynamic and aeroelastic responses of these plates are shown to be dependent upon the distribution of damage. The stress field within the laminae of the composite plate varies spatially and temporally due to the presence and distribution of the unsteady aerodynamic loads. As a consequence, the growth and distribution of damage are not uniform. The development of appropriate damage models is important as the change in the stress field affects the accumulation of damage and the resulting evolution of the aeroelastic stability boundaries. The results presented in this study verify that the stability characteristics must be identified for the evolving aeroelastic system. Furthermore, the modal and stability characteristics of the evolving structure will provide a nonevasive measure for damage detection and system identification.

## Acknowledgment

This research has been partially supported by Air Force Office of Scientific Research Grant F49620-92-J-0450; the authors wish to thank them for their support.

## References

[1]Dowell, E. H., *Aeroelasticity of Plates and Shells*, Noordhoff International, The Netherlands, 1975.

[2]Gray, C. E., Jr., Mei, C., and Shore, C. P., "A Finite Element Method for Large-Amplitude, Two-Dimensional Panel Flutter at Hypersonic Speeds," *AIAA Journal*, Vol. 29, No. 2, 1991, pp. 290–298.

[3]Dowell, E. H., "Fatigue Life Estimation of Fluttering Panels," *AIAA Journal*, Vol. 8, No. 10, 1970, pp. 1879–1881.

[4]Xue, D. Y., and Mei, C., "Finite Element Nonlinear Flutter and Fatigue Life of 2-D Panels with Temperature Effects," AIAA Paper 91-1170, April 1991.

[5]Chen, W. H., and Lin, H. C., "Flutter Analysis of Thin Cracked Panels Using the Finite Element Method," *AIAA Journal*, Vol. 23, No. 5, 1985, pp. 795–801.

[6]Kim, Y. I., and Strganac, T. W., "Aeroelastic Stability of Damaged Composite Structures," AIAA Paper 92-2392, April 1992.

[7]Strganac, T. W., Kim, Y. I., and Kurdila, A. J., "Nonlinear Flutter of Composite Plates with Damage Evolution," AIAA Paper 93-1546, April 1993.

[8]Strganac, T. W., and Mook, D. T., "A Numerical Model of Unsteady, Subsonic Aeroelastic Behavior," *AIAA Journal*, Vol. 28, No. 5, 1990, pp. 903–909.

[9]Albano, E., and Rodden, W. P., "A Doublet Lattice Method for Calculating Lift Distributions on Oscillating Surfaces in Subsonic Flows," *AIAA Journal*, Vol. 7, No. 2, 1969, pp. 279–285.

[10]Batina, J. T., "Efficient Algorithm for Solution of the Unsteady Transonic Small-Disturbance Equation," *Journal of Aircraft*, Vol. 25, No. 7, 1988, pp. 598–605.

[11]Ashley, H., and Zartarian, G., "Piston Theory—A New Aerodynamic Tool for the Aeroelastician," *Journal of the Aeronautical Sciences*, Vol. 23, No. 12, 1956, pp. 1109–1118.

[12]Kim, Y. I., "A Model for Dynamic and Aeroelastic Response of Composite Structures with Damage Evolution," Ph.D. Dissertation, Texas A&M Univ., College Station, TX, Dec. 1993.

[13]Coleman, B. D., and Gurtin, M. E., "Thermodynamics with Internal State Variables," *Journal of Chemical Physics*, Vol. 47, No. 2, 1967, pp. 597–613.

[14]Jones, R. M., *Mechanics of Composite Materials*, McGraw–Hill, New York, 1975.

[15]Talreja, R., "A Continuum Mechanics Characterization of Damage in Composite Materials," *Proceedings of the Royal Society of London*, Vol. A399, No. 1817, 1985, pp. 195–216.

[16]Talreja, R., "Stiffness Properties of Composite Laminates with Matrix Cracking and Interior Delamination," *Engineering Fracture Mechanics*, Vol. 25, Nos. 5–6, 1986, pp. 751–762.

[17]Allen, D. H., Harris, C. E., and Groves, S. E., "A Thermomechanical Constitutive Theory for Elastic Composites with Distributed Damage. Part I: Theoretical Development," *International Journal of Solids and Structures*, Vol. 23, No. 9, 1987, pp. 1301–1318.

[18]Allen, D. H., Harris, C. E., and Groves, S. E., "A Thermomechanical Constitutive Theory for Elastic Composites with Distributed Damage. Part II: Application to Matrix Cracking in Laminated Composites," *International Journal of Solids and Structures*, Vol. 23, No. 9, 1987, pp. 1319–1338.

[19]Allen, D. H., Groves, S. E., and Harris, C. E., "A Cumulative Damage Model for Continuous Fiber Composite Laminates with Matrix Cracking and Interply Delaminations," *Composite Materials: Testing and Design*, American Society for Testing and Materials, 1988, pp. 57–80.

[20]Harris, C. E., and Allen, D. H., "A Continuum Damage Model for Laminated Composite," *SAMPE Journal*, Vol. 24, Nos. 4–6, 1988, pp. 43–50.

[21]Lo, D. C., Allen, D. H., and Harris, C. E., "A Continuum Model for Damage Evolution in Laminated Composites," *Inelastic Deformations of Composite Materials*, edited by G. J. Dvorak, Springer–Verlag, New York, 1990, pp. 549–558.

[22]Sanders, D. R., Kim, Y. I., and Stubbs, N., "Nondestructive Evaluation of Damage in Composite Structures Using Modal Parameters," *Experimental Mechanics*, Vol. 32, No. 3, 1992, pp. 240–251.